A relation between ξ and θ along the wall surfaces is required and may be obtained by considering the geometry shown in Figure 1. If S is the x coordinate of the center of the circle involved, one may write

$$\tan\theta = \frac{y}{x - S} \tag{A8}$$

Substituting for x and y from Equations (3a) and (3b) into Equation (A8) and using the relations $S = S_1 = c \coth\alpha$ and $S = S_2 = c \coth\beta$ for the inner and outer circles, respectively, one obtains

$$\tan\theta)_{\substack{\text{inner}\\\text{wall}}} = \frac{\sinh\alpha \sin\xi}{\cosh\alpha \cos\xi - 1} \tag{A9}$$

$$\tan\theta)_{\substack{\text{outer}\\\text{wall}}} = \frac{\sinh\beta \sin\xi}{\cosh\beta \cos\xi - 1} \tag{A10}$$

Using the plus sign for the inner wall and the minus sign for the outer wall in Equation (A1) one gets

$$\tau_{\substack{\text{inner}\\\text{wall}}} = \tau_1 = \frac{\mu(1 - \cosh\alpha\cos\xi)}{r_1 \sinh\alpha\cos\theta} \frac{\partial u}{\partial\eta}\Big)_{\eta=\alpha} \tag{A11}$$

$$\tau_{\substack{\text{outer}\\\text{wall}}} = \tau_2 = \frac{-\mu(1 - \cosh\beta\cos\xi)}{r_2 \sinh\beta\cos\theta} \frac{\partial u}{\partial\eta}\Big)_{\eta=\beta} \tag{A12}$$

where θ and ξ along the walls are related through Equations (A9) and (A10). The average shear on each wall is given by

$$\tau_1)_{\text{avg}} = \bar{\tau}_1 = \frac{1}{\pi}\int_0^\pi \tau_1\, d\theta \tag{A13}$$

$$\tau_2)_{\text{avg}} = \bar{\tau}_2 = \frac{1}{\pi}\int_0^\pi \tau_2\, d\theta \tag{A14}$$

where the integration is performed over the range $0 \leq \theta \leq \pi$ because of symmetry about the x axis. From Equations (A11) to (A14), values of the ratio of local to average shear stress on each wall, namely $\tau_1/\bar{\tau}_1$ and $\tau_2/\bar{\tau}_2$, may be calculated.

Manuscript received May 5, 1964; revision received November 23, 1964; paper accepted November 25, 1964.

Normal Stress and Viscosity Measurements for Polymer Solutions in Steady Cone-and-Plate Shear

MICHAEL C. WILLIAMS

University of Wisconsin, Madison, Wisconsin

Normal stress and viscometric measurements were made on nine polymer solutions with cone-and-plate instruments. Temperature, concentration, molecular weight, and chemical structure were varied. Zero-shear viscosities, obtained by extrapolation of falling-sphere data, ranged from 0.7 to 380 poise.

A brief description is given of a normal stress-measurement apparatus, incorporating fast-response strain gauge pressure transducers. Measurements were made at shear rates between 5 and 2,800 sec.$^{-1}$, sometimes necessitating a considerable correction for inertial forces.

Non-Newtonian viscosity, normal stress, recoverable shear strain, and elastic modulus are presented in terms of modified Ferry reduced variables.

When viscoelastic liquids are subjected to shear, they exhibit a number of unique phenomena which distinguish them from so-called *Newtonian fluids*. Even in the restrictive case of steady viscometric flows studied here, their elastic properties give rise to non-Newtonian viscosity and various normal stress effects. In polymer solutions, such behavior is thought to be a consequence of cooperative configurational changes within and between solute molecules. These phenomena are currently the subject of considerable experimental investigation for the purposes of guiding engineering design, revealing the mechanical implications of fluid structure, and evaluating the many constitutive (rheological) equations which have been proposed.

The work reported here involved measurement of non-Newtonian viscosity and one normal stress function with cone-and-plate instruments. Supplementary information was obtained by falling-sphere viscosity tests.

CONE-AND-PLATE THEORY

Consider the geometry of Figure 1, in which a cone of radius R is rotating steadily with angular velocity Ω about an axis perpendicular to a stationary plate, and the cone vertex makes point contact with the plate. An incompressible fluid contained between the two surfaces is commonly assumed (5, 22) to flow in accordance with

Michael C. Williams is at the Institute of Theoretical Science, University of Oregon, Eugene, Oregon.

$$V_\phi = rw(\psi);\ V_r = 0;\ V_\psi = 0 \tag{1}$$

where $\psi = \pi/2 - \theta$ is the complement of the usual polar coordinate θ. Equation (1) satisfies identically the equation of continuity (5). If, furthermore, the angular spacing between surfaces is small, the equation of motion (5) reduces to the components

$$-\rho\frac{V_\phi^2}{r} = -\frac{\partial p}{\partial r} - \frac{\partial \tau_{rr}}{\partial r} + \frac{\tau_{\phi\phi} + \tau_{\psi\psi} - 2\tau_{rr}}{r} \tag{2}$$

$$0 = \frac{1}{r}\frac{\partial p}{\partial \psi} + \frac{1}{r}\frac{\partial \tau_{\psi\psi}}{\partial \psi} \tag{3}$$

$$0 = \frac{1}{r}\frac{\partial \tau_{\psi\phi}}{\partial \psi} \tag{4}$$

These lead ultimately to the excellent approximations for V_ϕ and shear rate γ:

$$V_\phi = r\,\Omega\,\psi/\psi_o \tag{5}$$

$$\gamma[\nabla V + (\nabla V)^T]_{\theta\phi} = -\cos\psi\frac{\partial}{\partial\psi}\left(\frac{V_\phi}{r\cos\psi}\right) = -\Omega/\psi_o \tag{6}$$

The constancy of γ implies that all purely shear-dependent stresses are also constant throughout the sheared fluid. These include the shear stress $\tau_{\psi\phi}$ and the normal stresses* $\tau_{\phi\phi}$, $\tau_{\psi\psi}$, and τ_{rr}.

The viscosity η can be measured through the relationship (5)

$$\eta \equiv -\tau_{\theta\phi}/\gamma = \tau_{\psi\phi}/\gamma = \left(\frac{3\psi_o}{2\pi R^3}\right) T/\Omega \tag{7}$$

where T is the torque required to rotate the cone. Normal stresses are described by Equation (2), which can be rewritten as

$$\frac{\partial \pi_{\psi\psi}}{\partial r} = \frac{\tau_{\phi\phi} + \tau_{\psi\psi} - 2\tau_{rr}}{r} + \rho\frac{V_\phi^2}{r} \tag{8}$$

because $\gamma_{\psi\psi}$ and τ_{rr} depend only on the constant γ

$$\frac{\partial \tau_{rr}}{\partial r} = 0 = \frac{\partial \tau_{\psi\psi}}{\partial r} \tag{9}$$

Here, $\pi_{\psi\psi} = p + \tau_{\psi\psi}$ is the total stress in the ψ direction, and is the quantity measured as indicated in Figure 1.

If Ω is sufficiently small, inertial stresses will be negligible. Equation (8) becomes

$$\frac{\partial \pi_{\psi\psi}}{\partial \ln r} = \tau_{\phi\phi} + \tau_{\psi\psi} - 2\tau_{rr} \equiv \chi \tag{10}$$

(The symbol χ will be used henceforth in this sense and as a material property will depend only on γ.) Experimental data plotted as $\pi_{\psi\psi}$ vs. ln r then produce a straight line with slope χ. However, stresses measured at high Ω will reflect the influence of the inertial term $\rho V_\phi^2/r$, even in the absence of secondary flows which might become important under extreme conditions (*11, 15, 26*). In this case, on integrating Equation (8) with respect to r, one obtains

$$\pi_{\psi\psi}(r, \psi; \Omega) + C(\psi; \Omega) = \int \frac{\chi}{r}\,dr + \rho\int\frac{V_\phi^2}{r}\,dr = \chi \ln r + \rho\,\Omega^2\left(\frac{\psi}{\psi_o}\right)^2\frac{r^2}{2} \tag{11}$$

In the limiting case of Newtonian fluids, $\chi = 0$, and according to Equation (11) one should find that $\pi_{\psi\psi}$ at $\psi = 0$ is a constant, independent of r for all Ω. Experimentally, however, an essentially parabolic radial inertial profile is always found (*14, 22, 25, 34*). Such a profile can be obtained by considering the physical measurement as an *average* stress. Integration of Equation (11) over the ψ coordinate $0 \leq \psi \leq \psi_o$ leads to

$$\overline{\pi_{\psi\psi}} + \overline{C} = \chi \ln r + \frac{1}{6}\rho\,\Omega^2 r^2 \tag{12}$$

This agrees with most data on inertial stresses in highly viscous Newtonian fluids (*14, 22, 25, 34*). The coefficient of r^2 is identical to that obtained by Greensmith and Rivlin (*14*) for the similar problem of flat disk rotation, although slightly different arguments were used. Equation (12) shows how an inertial correction may be applied to raw normal stress data to isolate χ from the total measurement. Further remarks on this problem appear elsewhere (*36*).

* The sign convention followed here is that positive normal stresses represent compression and negative stresses tension.

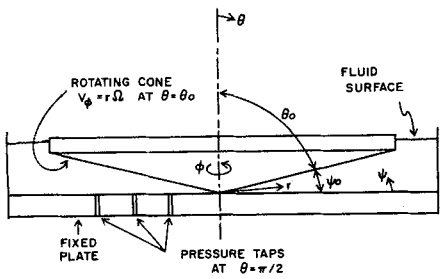

Fig. 1. Cone-and-plate geometry. Pressure taps shown here were present only in normal stress apparatus, not in viscometer.

EQUIPMENT

Falling Spheres

Low-shear viscosities were approximately determined from falling-sphere measurements (*32, 33*). Ruby spheres and steel ball bearings of diameters 0.025 to 1/16 in. were timed over a distance of 10.15 cm. in their center-line descent through fluid contained in a glass cylinder of diameter 4.72 cm. The cylinder was suspended in a temperature-regulated water bath with thermal control to ± 0.05°C.

Viscometer

A Ferranti-Shirley instrument, described in the literature (*24*), was used to determine non-Newtonian viscosities over a shear rate range of 10 to 18,000 sec.$^{-1}$. The cone had an angle of $\psi_o = 1/3$ deg. and diameter of 7 cm. It was found necessary to use the vapor shield to prevent solvent evaporation during test. Operating procedures were those recommended by Biery and Huppler (*4*). Isothermal conditions were achieved by circulation of water through the plate utilizing the same control system referred to above.

Normal Stress Apparatus

A cone-and-plate device was constructed along the general lines discussed by Markovitz (*20, 22, 23*). The cone angle was $\psi_o = 1$ deg. and cone diameter 5 in.

Two highly critical factors affecting data obtained from such an instrument are separation of the cone and the plate, and orientation of the plate surface. The former factor was controlled by adjustment of stops which permitted the cone assembly to be lowered only until a 1/1000-in. shim paper made grazing contact between the truncated (0.001 in.) cone tip and the plate. Plate orientation was fixed by judicious shimming and tightening of cap screws. This technique, checked with a sensitive indicator, kept the plate within 10^{-2} deg. of being perpendicular to the cone axis.

Four pressure taps of diameter 0.035 in. were drilled through the plate at azimuthal spacings of 90 deg. and at

radial positions 0.433, 0.708, 1.18, and 1.97 in. Each tap was connected by metal tubing to unbonded strain gauge pressure transducers below. During operation, the transducers contained water and the tubes contained the test liquid. Transducer voltage outputs were read from an oscilloscope.

This pressure-measuring system was limited in response speed primarily by the low-shear viscosity of the test samples, as the infinitesimal but nonzero volumetric displacement within the transducers was supplied by a creeping flow of test fluid. Whereas measurements with water and even glycerin came to equilibrium almost instantaneously, the more concentrated polymer solutions required times on the order of 30 min. This refers, of course, to equilibrium with the time-average pressure. It is doubtful that the measurements were always in equilibrium with transient fluctuations, clearly visible, which were caused by instrument imperfections and perhaps by liquid nonhomogeneity (*19*). An arithmetic mean of peak values of stress fluctuations was used in calculations.

One unexpectedly large source of such pressure fluctuations was found to be the two pillow-block bearings supporting the cone shaft. These permitted, or perhaps contributed, a vertical axial play of several ten-thousandths of an inch during rotation. A similar problem was encountered by Adams and Lodge (*1*). Such a movement sends pressure pulses through the liquid and is especially serious for highly viscous samples which cannot relieve the pulses by a flow mechanism. The problem was alleviated by axial spring loading of the rotating shaft against the upper pillow block, with the shaft then guided by a precision bearing with balls uniform to 10 millionths of an inch.

The drive system was powered by a D.C. motor connected to a variable-speed transmission, which in turn was coupled to the cone shaft via timing belt. Adjustment of motor speed and transmission setting permitted shear rates ($\gamma = 6 \times$ rev./min. of cone) of 3 to 3000 sec.$^{-1}$. Cone speeds were measured at low rates by an electric timer and at high rates by a tachometer.

Thermal control was secured to $\pm$ 0.05°C. by circulation of temperature-regulated water through a labyrinth of channels milled into the plate from below.

MATERIALS

Aqueous solutions* were prepared of polyethylene oxide (Polyox), hydroxyethyl cellulose (HEC), and polyvinyl alcohol (PVA). These linear polymers are identified more fully in Table 1. Molecular weights were supplied by the manufacturers except for HEC; in the latter case, the author's estimate is based on recent work (*12*) with a comparable grade of carboxymethylcellulose. Molecular weight in Table 1 is presumed to be a viscosity-average for Polyox and is a weight average for PVA.

Most solutions were prepared with moderate mechanical stirring, while powders were slowly added to distilled water; agitation was continued for hours beyond the point where apparent homogeneity was achieved. In the case of PVA, which was a highly hydrolyzed grade and therefore not very soluble, extreme shearing was necessary. Thus the PVA, and probably also the Polyox, which is known to be especially sensitive to shear (*7, 9*), underwent some mechanical degradation and reduction of molecular weight.

Isopropanol was mixed into all Polyox solutions to prevent oxidative aging (*7*); concentrations given here include the presence of this additive. Trace quantities of acetic acid were also added, just before testing, to dissolve residual salts and thus clarify the liquids to the point where falling spheres could be seen easily. The resulting solutions were found to be stable when kept under refrigeration at 5°C.

Solutions of HEC were preserved with traces of formalin and were extremely stable. Solutions of PVA contained no additives.

During preparation and handling, most of these fluids demonstrated characteristics of high elasticity, including the Weissenberg climbing effect, bubble recoil, jet swelling in transfer by hypodermic, and stringiness when touched. The latter has been associated with polydispersity of molecular weight (*7, 34*), and was particularly evident in P301 solutions.

* The experimentalist beginning a study of water-soluble resins is referred to the recent informative survey by Davidson and Sittig (*7*).

TABLE 1. IDENTIFICATION OF POLYMERS AND THEIR SOLUTIONS

Polymer	Molecular weight	Notation	Solution concentration, %	η_o, poise, at T°C.
Polyox, WSR-301 (Union Carbide)	40×10^5	P301	1.00	25.8 -25
			1.53	156.0 -15
			1.53	97.0 -25
			1.53	63.0 -35
			2.00	380.0 -25
Polyox, WSR-205	6×10^5	P205	2.00	0.69-25
			5.63	79.5 -25
Natrosol 250—high viscosity grade (Hercules)	3.5×10^5	HEC	1.54	218.0 -25
Elvanol 72-51 (Du Pont)	1.6×10^5	PVA	8.0	8.3 -25

DATA ANALYSIS AND RESULTS

Falling Spheres

The object of the falling-sphere experiment is to determine η_o, the zero-shear viscosity. There seemed to be no rigorous way of calculating this quantity directly from experimental data, since most of the test fluids exhibited elasticity and shear-dependent viscosity even for the slowest sphere descents.

These difficulties were surmounted by extrapolation of the raw data to zero-shear conditions; in this limit, Newtonian correction factors could be assumed valid. Extrapolation was performed with the parameters $\eta_o^{(N)}$ and $\tau_m^{(N)}$

$$\eta_o^{(N)} \equiv \eta_s f_w f_B f_I = [D^2(\rho_s - \rho)g/18V_t]\, f_w f_B f_I \quad (13)$$

$$\tau_m^{(N)} \equiv \frac{1}{6} Dg\,(\rho_s - \rho) \quad (14)$$

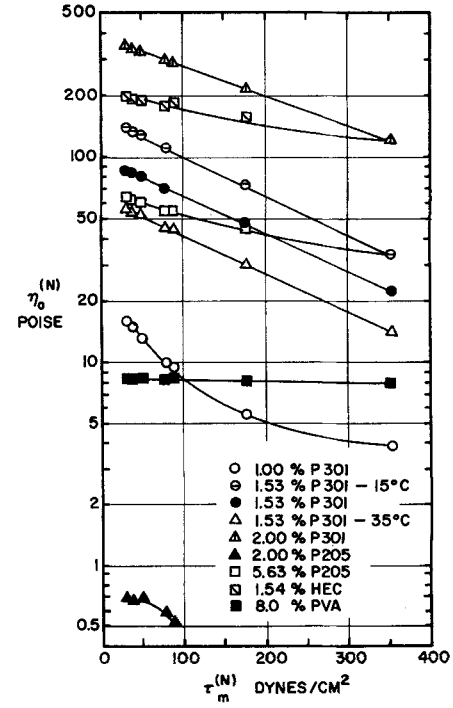

Fig. 2. Pseudo Newtonian viscosity $\eta_o^{(N)}$ as a function of pseudo Newtonian shear stress $\tau_m^{(N)}$, as determined by falling spheres. Temperature is 25°C. except where noted.

where $\tau_m^{(N)}$ is the maximum shear stress which would exist at the sphere surface if the fluid were Newtonian. The Stokes viscosity η_s and the correction factors for wall, bottom, and inertial effects (33)

$$f_W = 1 - 2.10\,(D/D_c) + 2.09\,(D/D_c)^3 - \ldots \quad (15)$$

$$f_B = 1/(1 + 1.65\,D/h) \quad (16)$$

$$f_I = 1/(1 + 3\,Re/16 - \ldots) \quad (17)$$

are valid only for Newtonian fluids. In Equation (17) $Re = DV_t\rho/\eta_s$ is a Reynolds number. Data then appeared as seen in the semi-log plot of Figure 2. Extrapolation to $\tau_m^{(N)} = 0$, either directly from Figure 2 or from a plot of $\eta_o^{(N)}$ vs. $[\tau_m^{(N)}]^x$, led to an intercept identified as η_o. The values so obtained are listed in Table 1.

In one instance, these data support the familiar relationship (*10, 27*)

$$\frac{\eta_o^{(i)}}{\eta_o^{(k)}} = \left(\frac{M_i}{M_k}\right)^{3.4} \quad (18)$$

which is often observed and can be predicted theoretically for entangled polymer systems such as melts and concentrated solutions. The data for P301 and P205 at 2.00% concentration can be fitted with an exponent of 3.33 into an equality like Equation (18), which suggests that the experimentally elusive zero-shear limit was indeed obtained by the procedures described above.

For some tests of Polyox solutions, a very slight regular lateral wobble seemed to accompany the sphere descent. This might be the spiralling-sphere phenomenon now being investigated by Shafrir (*29*), which is possibly related to the spiral motion of ascending bubbles (*6*), although most Reynolds numbers were extremely low in the present work. This raises interesting questions about mechanical stability in flow involving highly viscoelastic fluids.

Non-Newtonian Viscosity

The Ferranti-Shirley data can be presented compactly in terms of the reduced variables introduced by Ferry (*10*) and modified as in (*8*) and (*21*):

$$\eta_r \equiv \eta/\eta_o \quad (19)$$

$$\gamma_r \equiv \gamma(\eta_o/\eta_{or})\,(T_r/T)\,(c_r/c)^2 \quad (20)$$

The arbitrary reference quantities η_{or}, T_r, c_r are assigned values of 1 poise, 298°K., and 1%, respectively. Data for all nine fluids can then be represented on a single graph, Figure 3. Some data points have been omitted where overlap of distinct curves would occur.

Normal Stress

The transducer measurement of $\overline{\pi}_{\psi\psi} = \overline{p} + \tau_{\psi\psi}$ during steady shear includes contributions from the static pressure $\pi_{\psi\psi}(\Omega = 0) \equiv p_o$ and from fluid inertia $\overline{\mathcal{P}}_I$. These two pressures can be eliminated by the calculation of a corrected stress π_c

$$\pi_c \equiv \overline{\pi}_{\psi\psi} - p_o - \overline{\mathcal{P}}_I \quad (21)$$

which is then assumed to represent solely an elastic effect. $\overline{\mathcal{P}}_I$, in principle obtainable from Equation (12), was measured for a Newtonian liquid (95% glycerin, with $\rho = 1.2$ g./cc. and $\eta_o = 3.4$ poise). Values of $\overline{\mathcal{P}}_I(\Omega)$ for the elastic liquids were then taken from a smoothed curve representing the glycerin data, adjusted for density differences (1/1.2), and applied to $\overline{\pi}_{\psi\psi}$ at each pressure-tap position.

As is customary in normal stress work, $\overline{\pi}_{\psi\psi}$ was measured for both directions of cone rotation and then averaged.

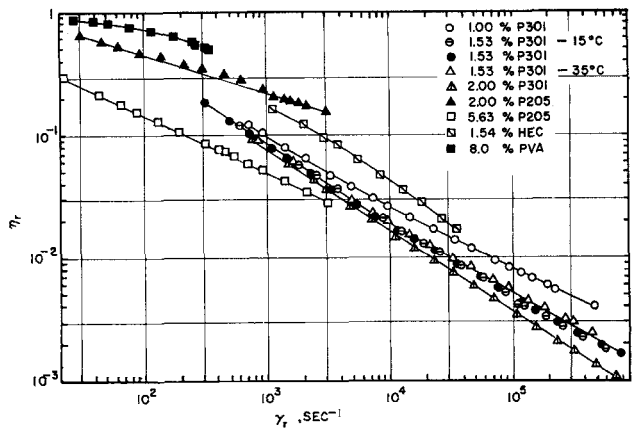

Fig. 3. Reduced viscosity η_r vs. reduced shear rate γ_r, at 25°C. except where noted.

This procedure was proposed (*14, 23*) in an effort to eliminate spurious pressures arising from imperfect alignment of the instrument or various hydrodynamic edge effects. For example, if the plate is not perpendicular to the cone, the fluid in passing over a given position will experience converging flow in clockwise rotation and diverging flow in counterclockwise rotation. To a certain extent, the averaging process eliminates such an effect (for small misalignments). Clearly, though, the extreme positions along the plate surface, one high and the other low, will still experience net effects of converging and diverging motion, as well as net shear rates higher and lower, respectively, than the desired one. This has been nicely demonstrated recently by Adams and Lodge (*1*), and present experience corroborates them.

Representative samples of such averaged values of π_c are given in Figure 4. The importance of $\overline{\mathcal{P}}_I$ is shown in Figure 4*b* for a fluid exhibiting rather low elastic stresses; the dotted line represents uncorrected data. Note that the corrected curve is not only elevated but also linearized with respect to ln r.

Slopes of the lines π_c vs. ln r lead to χ [see Equation (12)] which can be presented in reduced-variable form:

$$\chi_r = \chi(T_r/T)\,(c_r/c)^2 \quad (22)$$

Figures 5 and 6 exhibit such data for all nine fluids. Similar reduced plots appear in the work of Tamura, Kurata, and Kotaka (*30*) and Markovitz and co-workers (*21, 23*).

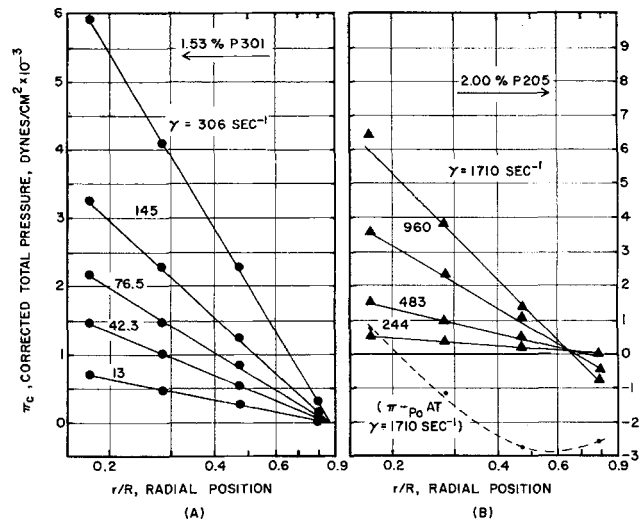

Fig. 4. Corrected total pressure π_C vs. $\log_{10}(r/R)$, at 25°C., for two fluids at several values of shear rate.

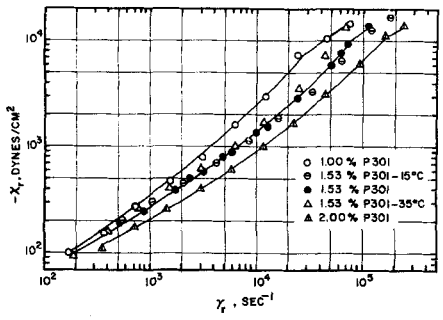

Fig. 5. Reduced normal stress function χ_r vs. reduced shear rate γ_r, for P301 solutions. Temperature is 25°C., except where noted. The middle line represents 1.53% P301 only at 25°C.

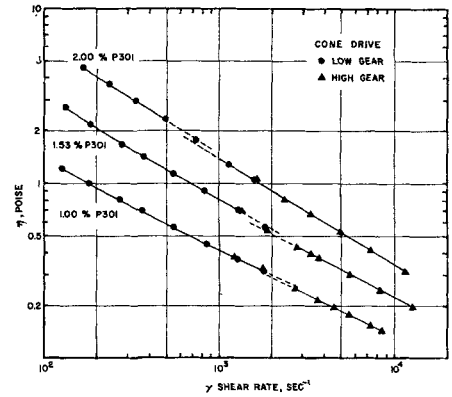

Fig. 7. Viscosity anomaly, shown as viscosity η vs. shear rate γ for P301 solutions at 25°C. Data for 1.53% P301 at 15° and 35°C. are consistent but are omitted for clarity. Dotted lines emphasize magnitude of the anomaly, which was ignored in drawing the smoothed curves of Figure 3. The transition at $\gamma = 1{,}800$ sec.$^{-1}$ from low to high gear of the viscometer drive was initially suspected of influencing the data, but these three curves seem to disprove such a contention.

DISCUSSION

Viscosities

Most of the fluids tested here were far from Newtonian, as evidenced by Figures 2 and 3. Only for 2.0% P205 and 8.0% PVA could this limit even be approached in the Ferranti-Shirley instrument.

As is well known (*10, 27*), non-Newtonian behavior in polymer solutions is accented by high molecular weights and concentrations of solute molecules. These characteristics seem to favor establishment of γ-dependent dynamic structural networks in the flowing fluid, due to long-range molecular entanglements (*8, 10, 18, 37*). Qualitatively, then, the nearly Newtonian PVA and 2% P205 may be thought to have little network structure [or possibly γ-independent structure (*18*)]. For its relatively modest molecular weight, the 1.54% HEC seems to possess rather well-developed structure; apparently the greater stiffness of the cellulosic molecule contributes to formation of entanglement networks (*10*, p. 192).

These reduced variables do not lead to a master plot of η_r for all materials but tend to isolate the behavior of each type of molecule. Thus data for P301 at three concentrations and three temperatures lie nearly together, while data for other polymers are significantly displaced. Even for the same molecules, however, all high-shear data will not commonly coincide in these variables because of the differences in the high-shear limits $\eta_{\infty r} = \eta_\infty/\eta_o$. Thus the superposition of data found possible in so many linear viscoelastic tests (*10*) seems unlikely in the general nonlinear case.

One peculiarity is noticeable in all the Polyox viscosities. At some shear rate between 500 and 3,500 sec.$^{-1}$, depending on the fluid, η experiences a slight but rather abrupt drop after which it continues with a different slope (Figure 7). This phenomenon was reproducible, with increasing or decreasing cone speed. Such behavior was never encountered with HEC, tested many times as a control. Based on the assumption that Polyox solutions have a unique network structure which can be disrupted at a critical shear stress τ^*, Table 2 was prepared. The constancy of τ^*/c values suggests that each polymer can be characterized by its own intermolecular cohesive energy per unit mass in solution. This would reflect how tightly the molecules form entanglements and associations.

A similar anomaly in cone-and-plate flow has been reported for viscoelastic bentonite suspensions (*13*).

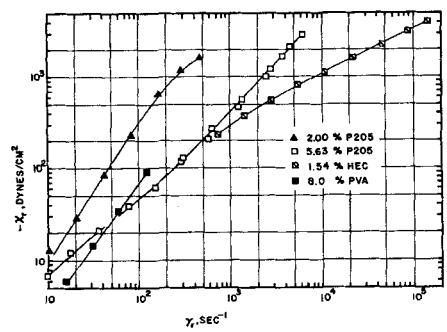

Fig. 6. Reduced normal stress function χ_r vs. reduced shear rate at γ_r, at 25°C.

Normal Stresses

The success of reduced variables in correlating normal stress data is comparable to their success for viscosities, with the divergent trends qualitatively the same.

As was generally the case also for viscometry, shear rates sufficiently low to permit measurement of limiting stress behavior could not be attained. But the data for one fluid shows unexpected behavior at the lowest shear rates achieved here. The 8% PVA exhibited normal stresses proportional to $\gamma^{1.6}$ over the same shear conditions for which its shear stresses were nearly proportional to $\gamma^{1.0}$ (viscosity almost Newtonian). This is contrary to expectations that the low-shear limiting normal stresses

TABLE 2. STRESS ANOMALIES IN POLYOX SOLUTIONS, 25°C.

Polymer	c, concentration g. cm.$^{-3}$	Shear stress anomaly† η, poise	γ, sec.$^{-1}$	τ^*, dyne cm.$^{-2}$	erg. g.$^{-1}$ τ^*/c	Normal stress anomaly‡ sec.$^{-1}$ γ,	cm.$^{-2}$ χ, dyne
P301	0.0200	2.3	495	1,140	57,000	1,700	43,000
	0.0153	0.70	1,300	910	59,500	1,700	22,000
	0.0100	0.32	1,800	575	57,500	1,100	7,500
P205	0.0563	3.4	560	1,900	33,800	—	—
	0.0200	0.19	3,500	665	33,200	—	—

† The quantity τ was estimated as $\tau_{\psi\phi}$ at the last experimental data point before the anomaly occurred (as $\tau_{\psi\phi}$ was being increased).

‡ These values of χ correspond to the breaks in Figure 5.

should vary with γ^2 and is reminiscent of the behavior reported for oscillatory stress measurements in solutions of polyisobutylene (8) in which the limiting storage modulus G' was found proportional to the 1.5 power of frequency.

In general, Figures 3 and 6 indicate that the nearly Newtonian fluids, characterized here as having little network structure, display normal stresses with a much different shear dependency than those of fluids with much structure. The latter not only have larger χ but also exhibit a semiplateau of normal stress at moderate shear which eventually increases to a near-linear dependence on γ. This high-shear behavior has been detectable to a lesser extent in a few other works (*20, 25, 30*).

The apparent break in the P301 data of Figure 5 at high shear (deliberately emphasized by the smoothed curves) cannot be satisfactorily explained at present. It it not obviously related to the viscosity anomaly, although it occurs in the same general range of γ, because its shear rate progression with solute concentration is in the opposite direction (see Table 2). Tests with Newtonian liquids also revealed peculiarities at roughly the same γ, suggesting an instrument or fluid instability, perhaps the onset of inertial secondary flows.

This phenomenon may be considered in another fashion, suggested by Figure 8, which displays the recoverable shear strain

$$s \equiv -\chi/\tau_{\psi\phi} \qquad (23)$$

For PVA and HEC, s is well behaved. But for the Polyox solutions, an abrupt (here exaggerated) change of slope appears at high γ. This strongly resembles the behavior of s_T, a recoverable shear defined for tube flow and possibly related to inlet effects (2, 3). In tubes a mechanism of flow instability is often invoked to explain the break in the s_T curve. The cone-and-plate phenomenon might also be thought to represent an instability, but whether the fundamental cause is fluid slippage at the cone surface, common shear degradation of the polymer, or actual fracture is not clear. It is observed that values of s at which the breaks occur in Figure 8 are closely approximated by

$$s_b = 0.1\sqrt{cM} \qquad (24)$$

with c in weight fraction and M = molecular weight.

ELASTIC MODULUS

Another means of presenting combined normal and shear stress information is through a fluid elastic modulus

$$G \equiv \tau_{\psi\phi}/s \qquad (25)$$

When a reduced modulus

$$G_r \equiv G\,(c_r/c)^2 \qquad (26)$$

is used, the data appear as shown in Figure 9. These curves have several interesting implications.

The conglomeration of points representing P301 at three concentrations and three temperatures defines a single curve. This reinforces the contention of DeWitt and co-workers (8) that c^2 is a significant reducing factor when describing fluids with a network structure. Furthermore, it facilitates prediction of P301 behavior at other temperatures and concentrations and may indicate that a similar correlation is possible for other materials. The P205 data are not a good test of this because the viscosity measurements were somewhat unreliable at 2.0% concentration.

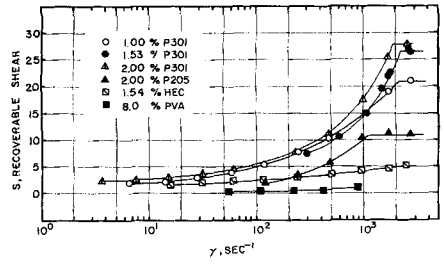

Fig. 8. Recoverable shear strain s vs. shear rate γ, at 25°C.

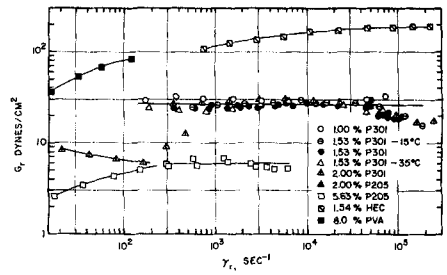

Fig. 9. Reduced shear modulus G_r vs. reduced shear rate γ_{r_r} at 25°C. except where noted. The departure of P301 data from the horizontal curve at high γ is a manifestation of the stress anomalies.

It is also notable that the P301 curve is nearly constant at a value of 25 to 30 dynes/sq. cm., over an immense range of γ. Examination of the other data suggests that such a plateau is actually a high-shear limiting characteristic for all polymer solutions. For fluids with considerable entanglement structure, such as the P301 solutions, this limit appears at rather low shear rates. The extent to which the G plateau is achieved determines the success of the power-law approximation (*31*); that is, if $\tau_{\psi\phi}$ is proportional to γ^n, then χ should be proportional to γ^{2n}:

$$-\chi \equiv s\tau_{\psi\phi} \equiv \tau^2_{\psi\phi}/G \doteq (m\gamma^n)^2/\text{const} \sim \gamma^{2n} \qquad (27)$$

SUMMARY

Cone-and-plate measurements of normal stress and shear stress in nine aqueous polymer solutions have demonstrated the influence of temperature, solute concentration, and solute molecular weight. These normal stress data were extended to shear rates appreciably higher than those reported for previous measurements with rotational apparatus. This necessitated a significant correction for inertial effects. Most of the analysis given here is rather routine, although the technique described for obtaining η_o may be novel. Additional analysis and interpretation will be the subject of another publication (36).

Polyethylene oxide, given primary attention, has never been the subject of a normal stress investigation, to the best of this writer's knowledge. It is of particular interest because of its water solubility, high molecular weight, and considerable elasticity in solution. Solutions of PVA (of a different grade than was used here) have been studied by Sakiadis (28) in the tube geometry, and HEC solutions have been investigated also by Meter (25) in a cone-and-plate instrument.

The general art of steady shear normal stress determination seems now to be in a state comparable to viscometry, allowing for errors and data scatter attending the measurement of a higher order phenomenon. Designers and theoretical rheologists may now refer to several sources for sound normal stress data (*1, 17, 20, 21, 30, 34*), although a need still exists for combined viscosity-normal stress information on *well-characterized* polymers. Further improvements are needed in most apparatus to eliminate the differences between pressures measured during clockwise and counterclockwise rotation, as well as the sur-

prisingly large time-dependent pressure fluctuations. The latter were never reported and probably unsuspected in early normal stress work because manometer response was far too slow. Manometric data undoubtedly represented a time average of such fluctuations. A similar criticism may be made of the present technique for averaging. Indeed, the very existence of such fluctuations will contribute to spuriously high average pressures (*35*) which could be especially undesirable at low shear rates. This might account for the $\gamma^{1.5}$ normal stress dependence found here in Newtonian polymer fluids, rather than the theoretically predicted γ^2 dependence. These problems must be solved before experimental studies of time-dependent normal stress behavior are undertaken (*35*).

ACKNOWLEDGMENT

The author wishes to thank Professor R. Byron Bird (University of Wisconsin) for guidance and stimulation throughout this project; Mr. T. W. Spriggs for aid in acquiring experimental data; and Dr. R. M. Turian for use of his falling sphere equipment.

The financial assistance of the National Science Foundation, through research grant G-11996 and four years of Cooperative Graduate Fellowships, is gratefully acknowledged.

NOTATION

c = weight concentration of polymer solute, % or fraction
$C, \bar{C}$ = constants of integration, Equations (11) and (12)
D, D_c = diameters of sphere and cylinder, cm.
g = gravitational constant, cm./sec.
G, G_r = elastic shear modulus for liquids and reduced modulus, dynes/sq. cm.
G' = storage modulus used to describe oscillatory testing, dynes/sq. cm.; see (*10*)
h = height above cylinder bottom, cm.
m, n = constants in the power-law rheological model
M = molecular weight
M_i, M_k = molecular weights of polymer homologs i and k
p, p_o = isotropic component of the stress and its static value, dynes/sq. cm.
$\mathcal{P}_I$ = dynamic contribution of inertial forces to the total stress, dynes/sq. cm.
r = radial coordinate, cm.
R = cone radius, cm.
s, s_T = recoverable shear strain, Equation (23); also defined in tube flow
s_b = value of s at break in Figure 8
$\mathcal{T}$ = torque resisting cone rotation, dyne cm.
T = temperature, °C. or °K.
V_i = velocity component in i direction, cm./sec. ($i = \phi, \psi, r$)
V_t = terminal descent velocity
x = exponent of $\tau_m^{(N)}$ used in extrapolation technique

Greek Letters

γ, γ_r = shear rate and reduced shear rate, sec.$^{-1}$
η, η_r = viscosity, poise, and reduced viscosity
η_o = zero-shear (Newtonian) viscosity, poise
$\eta_o^{(i)}, \eta_o^{(k)}$ = zero-shear viscosities of associated liquids
$\eta_o^{(N)}$ = pseudo Newtonian viscosity, from Equation (13), poise
θ, θ_o = usual polar angular coordinate, size of cone angle, rad.
π_{ik} = $p\delta_{ik} + \tau_{ik}$, total stress tensor, dynes/sq. cm.
ρ, ρ_s = mass density, g./cc., of liquid and of sphere, respectively; in high-polymer solutions, $\rho \doteq 1.0$
τ^* = value of $\tau_{\psi\phi}$ at break in viscosity, Figure 7
τ_{ik} = shear-stress (extra-stress) tensor, dynes/sq. cm.
$\tau_m^{(N)}$ = correlating parameter, Equation (14), dynes/sq. cm.
ϕ = azimuthal angular coordinate, rad.
χ = $\tau_{\phi\phi} + \tau_{\psi\psi} - 2\tau_{rr}$, normal stress function arising in cone-and-plate system, dynes/sq. cm.
ψ, ψ_o = $\pi/2 - \theta, \pi/2 - \theta_o$, rad.
Ω = rotational speed of cone, rad./sec.

LITERATURE CITED

1. Adams, N., and A. S. Lodge, *Phil. Trans. Royal Soc. (London)*, **A256**, 149 (1964).
2. Arai, T., and H. Aoyama, *Trans. Soc. Rheol.*, **7**, 333 (1963).
3. Bagley, E. B., *ibid.*, **5**, 355 (1961).
4. Biery, J., and J. D. Huppler, *Univ. Wisc. Exptl. Sta. Report No. 19*, Univ. Wisc., Madison, Wisconsin (1962).
5. Bird, R. B., W. E. Stewart, and E. N. Lightfoot, "Transport Phenomena," 2 printing, pp. 83, 86, 100, Wiley, New York (1962).
6. Birkhoff, G., "Hydrodynamics," revised ed., p. 39, Princeton University Press, Princeton, New Jersey (1960).
7. Davidson, R. L., and M. Sittig, ed., "Water-Soluble Resins," Reinhold, New York (1962).
8. DeWitt, T. W., H. Markovitz, F. J. Padden, and L. J. Zapas, *J. Colloid Sci.*, **10**, 174 (1955).
9. Fabula, A. G., *Trans. Soc. Rheol.*, **8**, in press.
10. Ferry, J. D., "Viscoelastic Properties of Polymers," Wiley, New York (1961).
11. Giesekus, H., "Proceedings of the Fourth International Congress Rheology," Interscience, New York, forthcoming publication.
12. Goring, D. A., and G. Sitaramaiah, *Polymer*, **4**, 7 (1963).
13. Gotch, R., T. Hanai, and H. Aidi, *J. Jap. Soc. Test. Matl.*, **11**, 285 (1962); see ref. in *Rheol. Abst.*, **6**, 26 (March 1963).
14. Greensmith, H. W., and R. S. Rivlin, *Phil. Trans. Roy. Soc. (London)*, **A245**, 399 (1953).
15. Hoppmann, W. H., II, and C. E. Miller, *Trans. Soc. Rheol.*, **7**, 181 (1963).
16. Jobling, A., and J. E. Roberts, *J. Polymer Sci.*, **36**, 421, 433 (1959).
17. Kotaka, T., M. Kurata, and M. Tamura, *J. Appl. Physics*, **30**, 1705 (1959); also *Rheol. Acta*, **2**, 179 (1962).
18. Lodge, A. S., *Trans. Faraday Soc.*, **52**, 120 (1956).
19. ———, *Polymer*, **2**, 195 (1961).
20. Markovitz, H., *Trans. Soc. Rheol.*, **1**, 37 (1957).
21. ———, and D. Brown, *ibid.*, **7**, 137 (1963).
22. ———, "Proceedings International Symposium on Second-Order Effects," Jerusalem Academic Press, Haifa, Israel (1964).
23. Markovitz, H., and B. Williamson, *Trans. Soc. Rheol.*, **1**, 25 (1957).
24. McKennell, R., *Anal. Chem.*, **28**, 1710 (1956).
25. Meter, D. M., Ph.D. thesis, Univ. Wisc., Madison, Wisconsin (1963).
26. Miller, C. E., and W. H. Hoppmann, II, *Trans. Soc. Rheol.*, **8**, in press.
27. Porter, R. S., and J. F. Johnson, *ibid.*, **7**, 241 (1963); also **6**, 107 (1962).
28. Sakiadis, B. C., *A.I.Ch.E. Journal*, **8**, 317 (1962).
29. Shafrir, U., *Sci. Amer.*, **210**, 71 (February, 1964).
30. Tamura, M., M. Kurata, and T. Kotaka, *Bull. Chem. Soc. Jap.*, **32**, 471 (1959).
31. Tomita, Y., *Bull. Jap. Soc. Mech. Eng.*, **2**, 469 (1959).
32. Turian, R. M., Ph.D. thesis, Univ. Wisc., Madison, Wisconsin (1964).
33. Van Wazer, J. R., J. W. Lyons, K. Y. Kim, and R. E. Colwell, "Viscosity and Flow Measurements," Interscience, New York (1963).
34. Williams, M. C., Ph.D. thesis, Univ. Wisc., Madison, Wisconsin, (1964).
35. ———, and R. B. Bird, *Ind. Eng. Chem.-Fund.*, 3, 42 (1964).
36. Williams, M. C., *Chem. Eng. Sci.*, to be published.
37. Yamamoto, M., *J. Phys. Soc. Jap.*, 13, 1200 (1958).

Manuscript received August 12, 1964; revision received December 15, 1964; paper accepted December 17, 1964.